Protein engineering of α-ketoisovalerate decarboxylase for improved isobutanol production in *Synechocystis* PCC 6803

Rui Miao, Hao Xie, Felix M. Ho, Peter Lindblad*

Microbial Chemistry, Department of Chemistry-Ångström Laboratory, Uppsala University, Box 523, SE-751 20 Uppsala, Sweden

A B S T R A C T

Protein engineering is a powerful tool to modify *e.g.* protein stability, activity and substrate selectivity. Heterologous expression of the enzyme α-ketoisovalerate decarboxylase (Kivd) in the unicellular cyanobacterium *Synechocystis* PCC 6803 results in cells producing isobutanol and 3-methyl-1-butanol, with Kivd identified as a potential bottleneck. In the present study, we used protein engineering of Kivd to improve isobutanol production in *Synechocystis* PCC 6803. Isobutanol is a flammable compound that can be used as a biofuel due to its high energy density and suitable physical and chemical properties. Single replacement, either Val461 to isoleucine or Ser286 to threonine, increased the Kivd activity significantly, both *in vivo* and *in vitro* resulting in increased overall production while isobutanol production was increased more than 3-methyl-1-butanol production. Moreover, among all the engineered strains examined, the strain with the combined modification V461I/S286T showed the highest (2.4 times) improvement of isobutanol-to-3M1B molar ratio, which was due to a decrease of the activity towards 3M1B production. Protein engineering of Kivd resulted in both enhanced total catalytic activity and preferential shift towards isobutanol production in *Synechocystis* PCC 6803.

1. Introduction

Using different microorganisms to produce valuable compounds has been investigated intensively during the last decades (Du et al., 2011; Nozzi et al., 2013; Lee and Kim, 2015; Chew et al., 2017). Diverse approaches like codon optimization (Redding-Johanson et al., 2011), transcriptional engineering (Du et al., 2012; Huang et al., 2010) and translational engineering (Nowroozi et al., 2014), can be applied to improve the performance of targeted metabolic pathway(s) and product (s). However, numerous limitations, especially relating to enzyme stability, kinetics, cofactor preference and substrate selectivity, cannot be overcome by using the above-mentioned strategies (Eriksen et al., 2014). Hence, protein engineering is a useful tool to modify and change the characteristics of enzymes, thereby overcoming the obstacles on protein level and optimize the flux in the target pathway.

Directed evolution is a powerful method for protein engineering which mimics natural evolution (Arnold and Volkov, 1999). Random mutants are generated using error-prone PCR, DNA shuffling or chemical mutagenesis. This is followed by selection based on different enzyme characteristic parameters, *e.g.* substrate range, thermostability, and activity. However, this method requires a significantly large mutant library and high-throughput screening method, both of which are time

consuming to develop, even though this approach offers full mutation on the entire enzyme (Eriksen et al., 2014). In contrast, rational design (Arnold, 1993) minimizes the size of the mutant library by predicting which specific amino acid mutations may affect enzymatic properties based on *a priori* knowledge about the enzyme such as crystal 3D structure, position of activity site and utilization of cofactor (Eriksen et al., 2014).

A number of examples demonstrate that protein engineering deserves more attention since it is a highly efficient tool to modify the performance of metabolic pathway dramatically. For instance, a xylose reductase was successfully engineered to have significantly increased substrate preference towards D-xylose (Nair and Zhao, 2008) over L-arabinose. In another study, the ketoacyl-reductase (KR) domain of fatty acid synthase (FAS-B) was inactivated by mutating its key catalytic residues (Zha et al., 2004). As a result, the mutant lost the ability to utilize NADPH so the carbon flux was shifted towards the production of triacetic acid lactone (TAL) which can be synthesized by FAS-B under NADPH limited condition. Similarly, amino acid substitutions on the *Aeromonas caviae* R-specific enoyl-coenzyme A (enoyl-CoA) hydratase (PhaJ_AC) changed the substrate specificity significantly towards octenoyl-CoA compared to wild type (Tsuge et al., 2003).

The objective of the present study was to use a protein engineering

approach to modify the metabolic pathway and, thereby, enhance iso-butanol production in the unicellular cyanobacterium *Synechocystis* PCC 6803 (*Synechocystis*). Isobutanol has been produced in different microorganisms as a petroleum alternative compound with the highest titer of 50 g L^{-1}, reported for an engineered *E. coli* strain grown under batch bioreactor cultivation in combination with an *in situ* product removal process (Baez et al., 2011). In cyanobacteria, the keto acid pathway has been studied in *Synechococcus elongatus* PCC 7942 (*Synechococcus*) (Atsumi et al., 2009; Li et al., 2014; Shen and Liao, 2012; Jazmin et al., 2017) and *Synechocystis* (Varman et al., 2013; Miao et al., 2017). In our previous study, we demonstrated that due to the high catalytic efficiency of endogenous alcohol dehydrogenases in *Synechocystis*, 2-ketoisovalerate decarboxylase (Kivd) is the only heterologous enzyme needed to be introduced for direct isobutanol production in the cells. However, when introduced, it is a potential bottleneck in the isobutanol synthesis pathway in *Synechocystis* (Miao et al., 2017). In another study, it was also shown that Kivd plays an important role in isobutanol production *in Clostridium cellulolyticum* (*C. cellulolyticum*). The strain with the highest Kivd activity also showed the highest isobutanol production even if the activities for all other enzymes in the pathway were lower (Higashide et al., 2011).

Kivd, from *Lacococcus lactis* (*L. lactis*) IFPL730, is a thiamine diphosphate (ThDP)-dependent 2-keto acid decarboxylase that can utilize different substrates e.g. α-ketoisovalerate, α-ketoisocaproate, α-keto-methylvalerate, and α-phenylpyruvate. Kivd is a monocistronically transcribed protein that shares a high homology (40%) with in-dolepyruvate decarboxylase gene from *Enterobacter cloacae* (*E. cloacae*) and its active form is a homo-tetramer. The diphosphate group of ThDP settles in the active site of Kivd with the help of Mg^{2+} (Dobritzsch et al., 1998), and a conserved glutamate residue in Kivd supports the depro-tonation and ylide-form shaping of ThDP (Kern et al., 1997; Breslow, 1957). The Kivd catalyzed decarboxylation includes: the reaction between ylide-form ThDP and the carbonyl group of substrate, the generation of active aldehyde after the release of CO_2, the protonation of the enamine intermediate, and in the end, the release of the corresponding aldehyde (Frank et al., 2007; Kluger, 1987) (Fig. 1).

Since Kivd can utilize multiple substrates, structural engineering of this protein has been done for non-natural long chain alcohols production in *Escherichia coli* (*E. coli*) and significant increase of C6 alcohol production was observed after enlarging the substrate binding pocket (Zhang et al., 2008). Similar reconstruction was performed on Kivd to enhance isovalerate and isocaproate production in *E. coli*, but unfortunately, the isocaproate titer increased only by a trace amount while the isovalerate titer decreased significantly (Xiong et al., 2012). Furthermore, saturated mutagenesis of Kivd was done for the production of 1-pentanol and higher substrate selectivity towards 1-pentanol precursor was achieved when substituted V461 to glycine or serine

(Chen et al., 2017).

Kivd introduced into *Synechocystis* results in two products, iso-butanol and 3-methyl-1-butanol (3M1B) (Miao et al., 2017). The substrate for isobutanol production (2-ketoisovalerate, KIV) contains one carbon less, *i.e.* is a smaller molecule, than the substrate for 3M1B production (2-ketoisocaproate, KIC). Here we investigated the feasibility of minimizing the substrate binding pocket size of Kivd in order to increase the activity and preferential shift towards the substrate KIV, and thereby increase the production of isobutanol.

2. Material and methods

2.1. Strains and cultivation conditions

Escherichia coli strain DH5αZ1 (Invitrogen) was used for cloning and conjugation work. The cells were grown at 37 °C in LB medium (agar or liquid) supplemented with 50 μg ml^{-1} kanamycin (Sigma-Aldrich). The glucose-tolerant *Synechocystis* PCC 6803 strain was used in this study. *Synechocystis* seed cultures were grown under 20 μmol photons m^{-2} s^{-1} at 30 °C in BG11 (Rippka et al., 1979) with addition of 50 μg ml^{-1} kanamycin. Experimental cultures were inoculated as OD$_{750}$ = 0.1 with a total volume of 25 ml in BioLite 25 cm^2 plug-sealed tissue culture flasks (Thermo Fisher Scientific). The medium was BG11 with addition of 50 μg ml^{-1} kanamycin and 50 mM NaHCO$_3$ (Sigma-Aldrich). The flasks were shaken horizontally at 120 rpm, under 50 μmol photons m^{-2} s^{-1} at 30 °C. 2 ml of culture was sampled from each flask every second day for OD$_{750}$ and products measurements while 2 ml fresh BG11 medium with addition of 50 μg ml^{-1} kanamycin and containing 500 mM NaHCO$_3$ was added back.

2.2. Plasmid construction

The self-replicating plasmid pEEK2-*kivd* (Miao et al., 2017) containing a strong constitutive promoter P*trc*$_{core}$ and codon optimized *kivd* was used as template to make the site-directed mutagenesis constructs in this study. Primers used in site-directed mutagenesis were listed in (Supplementary 1).

2.3. Conjugation of Synechocystis

E. coli cargo cells and *E. coli* HB101 helper cells with the plasmid pRL443-AmpR were grown overnight at 37 °C. The overnight cultures were centrifuged at 3000 rpm for 5 min and resuspended in fresh liquid LB medium without antibiotics. Wild-type *Synechocystis* cells (200 μl) were mixed with 1 ml cargo cells and 1 ml helper cells and the mixture was incubated under 100 μmol photons m^{-2} s^{-1} at 30 °C for 1.5 h before being spread on the filter on BG11 agar plate for another 48 h of
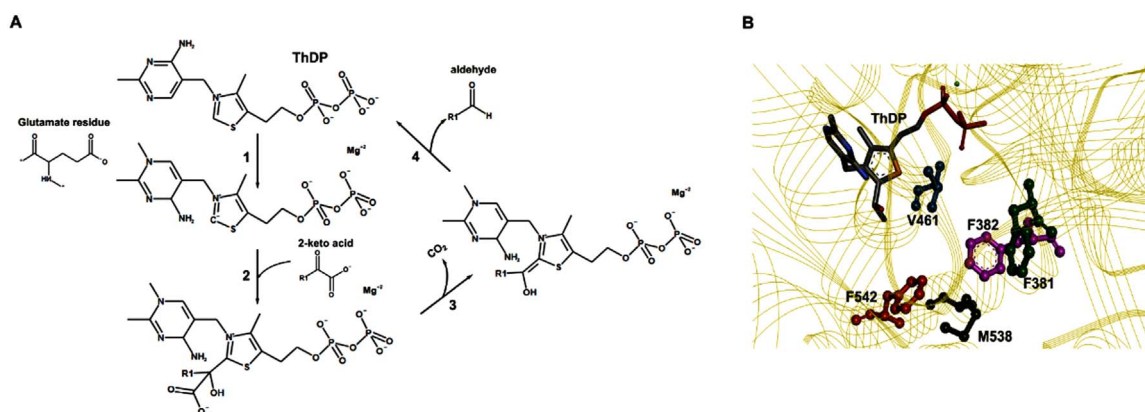

Fig. 1. Schematic of Kivd catalyzed decarboxylation reaction and residues in predicted Kivd active site. A) Kivd catalyzed decarboxylation: 1) Mg^{2+} helps ThDP to localize in the active site of Kivd while glutamate residue initiates the deprotonation of the pyrimidine ring on ThDP and form the active-conformation. 2) The activated ThDP reacts with the carbonyl group of substrate. 3) One CO_2 is released from the substrate. 4) Corresponding aldehyde is released from the complex and ThDP. B) Predicted Kivd active site structure.

incubation.

For colony selection and maintenance, the filters were changed onto new BG11 agar plates with $50\,\mu g\,ml^{-1}$ kanamycin. Gene specific primers were used to analyse the colonies and the correct colonies were inoculated into 6-well plates for further use.

2.4. Crude protein extraction and SDS-PAGE/Western-immunoblot

Proteins were extracted from day 2 cultures, cells were harvested by centrifugation at 5000 rpm, 4 °C, for 10 min. The pellet was washed in 2 ml PBS and recollected by centrifugation, 5000 rpm, 4 °C, for 10 min, and resuspended in 200 μl PBS with Protease Arrest (GBioscience). This mixture went through a freeze-thaw process and was disrupted by acid-washed 425–600 μm diameter glass beads (Sigma-Aldrich) using the Precellys-24 Beadbeater (Bertin Instruments), program $3 \times 30\,s$. Centrifugation was performed twice at 12,000 rpm, 4 °C, 1 min each, to get a clean supernatant containing soluble proteins. Protein concentration was determined by the DC protein assay (Bio-Rad). 4 μg soluble proteins from each strain were separated by SDS-PAGE, using Mini-PROTEAN TGX TM gels (Bio-Rad), and transferred to PVDF membrane (Bio-Rad). Anti-Strep-tag II (abcam) antibody was used to detect Strep-tagged Kivd through standard techniques while anti-ATPase Western-immunoblot was done one the same samples as loading control. This Western-immunoblot was repeated 3 times for determining the relative Kivd expression level in all the strains.

2.5. Kivd in vitro activity assay

The decarboxylation activity of Kivd using KIV was measured using a previously established coupled enzymatic assay method (Zhang et al., 2008) with several modifications. Kivd converts KIV into isobutyraldehyde and the NADH dependent ADH from *Saccharomyces cerevisiae* (*S. cerevisiae*) was used to reduce isobutyraldehyde into alcohol. Therefore, Kivd´s activity was measured by monitoring the NADH consumption at 340 nm at room temperature for 30 min using a spectrophotometer (Cary 50 Bio UV–visible spectrophotometer). Protein crude extract of each strain was normalized to a same concentration, $45\,\mu g\,\mu l^{-1}$, and 5 μl was used in the assay. The assay mixture contained 50 mM potassium phosphate (Sigma-Aldrich), 1 mM $MgSO_4 \cdot 7H_2O$ (Sigma-Aldrich), 0.5 mM thiamine pyrophosphate (Sigma-Aldrich), 0.2 mM NADH disodium salt (Roche Diagnostics), 0.1 μM ADH. The reaction was initiated by adding the substrate KIV (Sigma-Aldrich). The relative activity was calculated according to the relative Kivd expression level.

2.6. Optical density measurement and products quantification

Optical density was measured every day in 96-well plates using a micro-plate reader (HIDEX, Plate Chameleon). Every second day, 2 ml culture was sampled from each flask and centrifuged at 5000 rpm, for 10 min. 1305 μl of the supernatant was transferred into a 15 ml screw cap tube, mixed with 45 μl $3000\,mg\,L^{-1}$ internal standard, 1-pentanol, and 450 μl extraction solvent DCM. The mixture was shaken on Multi-Tube Vortexer VX-2500 (VWR) at maximum speed for 5 min and then centrifuged at 5000 rpm, 4 °C, for 10 min. DCM phase (bottom) was transferred into 1.5 ml clear glass gas chromatography (GC) vials (VWR). The extracted samples were analyzed on a PerkinElmer GC 580 system equipped with a flame ionization detector and an Elite-WAX Polyethylene Glycol Series Capillary column, $30\,m \times 0.25\,mm \times 0.25\,\mu m$ (PerkinElmer). Nitrogen was the carrier gas, with 10 ml/min flow rate. The temperatures of injector and detector were 220 °C and 240 °C, respectively. The initial oven temperature was 50 °C and then raised to 100 °C with a rate of $10\,°C\,min^{-1}$ followed by a rise to 180 °C with a rate of $20\,°C\,min^{-1}$. The GC results were analyzed using TotalChrom Navigator version 6.3.2.

3. Results and discussion

3.1. Residues selection for reforming the substrate binding pocket

The literature has shown that an *E. coli* mutant produced three times more longer chain alcohols compared to the wildtype when Val461 in Kivd was changed to alanine since the substrate binding pocket of Kivd was enlarged effectively (Zhang et al., 2008). Since the aim of our present study is to favour isobutanol production in *Synechocystis* by engineering Kivd to increase its efficiency towards isobutanol production precursor, the smaller substrate KIV, rather than the bigger substrate KIC that leads to 3M1B production, we hypothesized that reducing the substrate binding pocket could give the desired result. For this, a closer examination of the structure of Kivd was required in order to select the suitable residues for mutation. However, there is to our knowledge no crystal structure of Kivd available. Therefore, the structure of a crystallized branched-chain keto acid decarboxylase (Kdca) from *L. lactis* B1157 (PDB: 2vbg) (Berthold et al., 2007) was used as a model since these two enzymes share 88% amino acid sequence identity (Milne et al., 2015). In particular, sequence alignment showed that all the residues in the active site of Kivd (Phe381, Phe382, Val461, Met538, and Phe542 (Xiong et al., 2012)) are fully conserved in Kdca, so it is likely that the structure of the Kdca active site provides good indications of the structure of the Kivd active site, as well as the positioning of the activated V-shape cofactor ThDP nearby (Fig. 1B).

Based on this analysis, the two large residues Phe381 and Phe382 in Kivd are expected to be found with their phenyl rings next to each other, so it may be difficult to change either of them into a larger amino acid without causing significant problems with steric hindrance and possible detrimental deformation of the active site. Therefore, we focused on mutating the other three amino acids (V461, M538, and F542) in the active site in order to minimize the substrate binding pocket, and constructed the engineered strains V461I (VI), V461L (VL), V461F (VF), M538W (MW), F542W (FW). Moreover, we noticed that another two residues, Gln377 and Ser286, are close to the active site and may contribute to substrate selection and docking. Mutating these two amino acids to larger ones may result in reducing the size of the substrate binding pocket as well, so we constructed engineered strains Q377W (QW), S286T (ST), S286Y (SY). On the other hand, we also wanted to test the effect of enlarging the size of the substrate binding pocket of Kivd in *Synechocystis*. Hence, we changed Val461 and Ser286 to alanine and Phe542 to leucine generating the engineered strains V461A (VA), S286A (SA) and F542L (FL), respectively. In our previous study, it was demonstrated that the strain expressed only *kivd* on the self-replicating vector pEEK2 showed higher isobutanol production than the strains that co-expressed both *kivd* and a gene for alcohol dehydrogenase. Western-immunoblot analyses of these strains showed that the *kivd*-only strain had the highest Kivd expression level. Therefore, the same *kivd*-only self-replicating vector is also used in the present study to ensure a high level of Kivd expression. The omission of alcohol dehydrogenase genes in the vector is not a limiting factor in this study, since previous *in vivo* assay have confirmed the high catalytic efficiency of native *Synechocystis* alcohol dehydrogenases and will therefore not be a bottleneck for isobutanol production (Miao et al., 2017).

3.2. Isobutanol and 3M1B production and Kivd expression levels in different engineered Synechocystis strains

For the first step, we measured the total isobutanol and 3M1B titer from all the strains after cultivating the engineered *Synechocystis* strains for four days, in the plug-sealed tissue culture flasks (Fig. 2A). Strain ST showed dramatically increased titer for both products compared to the original Kivd strain and the isobutanol-to-3M1B titer ratio in this strain also increased. Moreover, strain SY produced lower amount of each product than the original strain, which indicates that the change from
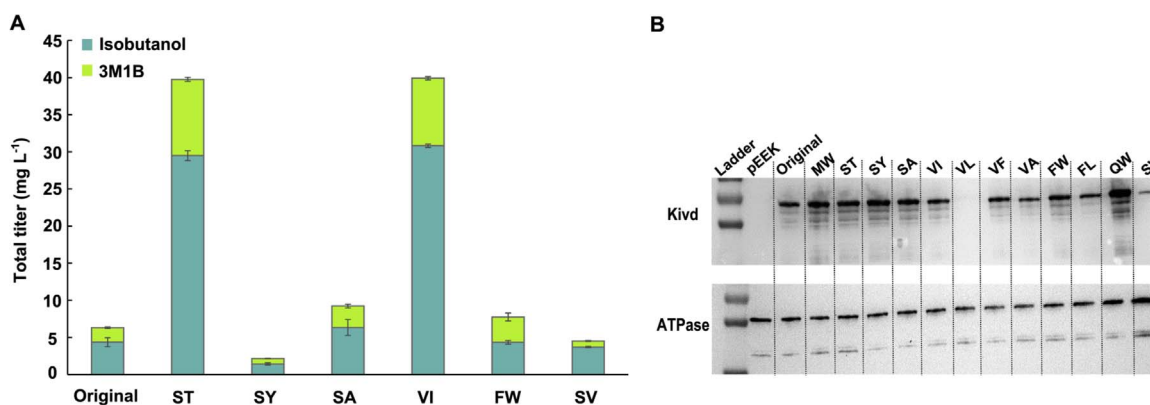
Fig. 2. Total titer of isobutanol and 3-methyl-1-butanol production and Kivd expression levels in different engineered *Synechocystis* PCC 6803 strains. A) Total titer of isobutanol and 3-methyl-1-butanol production from different engineered strains on day 4. The results for the 5 strains that did not produce the targeted products are not shown. Results represent the mean of three biological replicates, error bars represent standard deviation. B) Anti-strep tag Western-immunoblot to detect Kivd, anti-ATPase Western-immunoblot was used as loading control. pEEK is the empty vector control strain.
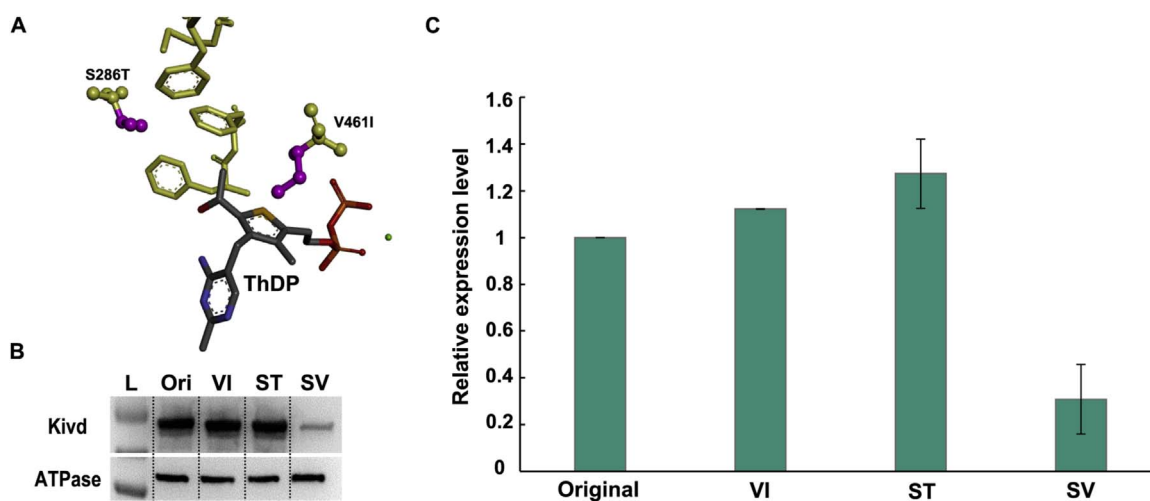

Fig. 3. Structure of the predicted active site of Kivd and relative expression level of different mutated Kivd in the selected engineered *Synechocystis* PCC 6803 strains. A) Mutations of the residues in the active sites of VI, ST and SV. The yellow residues are the unchanged ones and the violet parts are the differences between the original residues and the mutated residues. Strains VI and ST have the corresponding change and the combined strain SV has both. B) Anti-strep tag Western-immunoblot to detect Kivd, anti-ATPase Western-immunoblot was used as loading control. This Western-immunoblot was repeated three times. C) Relative expression levels of Kivd in different engineered strains. They were quantified based on band intensity on the Western-immunoblot images using QuantityOne software. Results represent the mean of three technical replicates with two biological replicates, error bars represent standard deviation.

Ser286 to tyrosine might be too disruptive since the sizes of these two amino acids differ too much. The additional phenyl ring on tyrosine might cause too much crowding for the residues nearby, and therefore be detrimental to the active site. The strain SA, which was made to investigate the effect of increasing substrate binding pocket, produced slightly more isobutanol and 3M1B while the isobutanol-to-3M1B titer ratio decreased compared to the original strain (Fig. 2A). All these results indicate that Ser286, which is currently not suggested as a part of the active site of the enzyme, is nevertheless an important amino acid for both the overall activity of Kivd and the preferential shift towards isobutanol production (Fig. 3A).

Another strain VI showed significant improvement on producing both isobutanol and 3M1B, and similar to strain ST, the isobutanol-to-3M1B titer ratio increased as well (Fig. 2A). This may due to the location of Val461, which is close to the thiazole ring on the cofactor ThDP (Fig. 3A). The enlargement of Val461 to isoleucine might help the substrate to anchor in the pocket in an appropriate position, making the interaction between the substrate and the cofactor easier. The importance of the residue V461 in both Kivd and KdcA has also been demonstrated in other studies (Zhang et al., 2008; Yep et al., 2006; Chen et al., 2017). However, interestingly, in the study from Chen et al., the substitution of V461 to isoleucine in Kivd did not showed any

improvement for the overall activity of the enzyme and the titer of the smaller products did not increase either. The different results from the same substitution in these two studies may due to the different substrate usage. The study from Chen et al. focused on the production of single-chain alcohols, so the branched-chain alcohol synthesis pathway was deleted in their *E. coli* strains, whereas both of the products that we could detect in our engineered *Synechocystis* strains are branched-chain alcohols, and both Kivd and KdcA were characterized as branched-chain keto acid decarboxylases, which means that they have much higher activities towards branched-chain substrates. Therefore, the effect of the engineered Kivd on the formation of branched-chain products may vary from the effects on single-chain products since the substrates have different steric natures.

Based on the good performance of VI and ST, we constructed strain SV containing a combined engineered Kivd S286T/V461I (Fig. 3A). As expected, a higher isobutanol-to-3M1B titer ratio was gained from this strain (Fig. 2A). However, surprisingly, the overall products formation from this strain was significantly lower compared to the original strain.

Strain FW showed increased 3M1B production and the same isobutanol production compared to the original strain. This was an unexpected result, given that the tryptophan residue is significantly larger than phenylalanine, and was expected to lead to less effective binding

of the larger KIC substrate in the binding pocket. However, there may have been other changes in the dimensional direction of the sidechain, leading to as yet unknown effects on the substrate binding pocket. Unfortunately, neither isobutanol or 3M1B was detected as product from the strains MW, VL, VF, VA, FL, and QW.

In order to investigate the reasons for low production or no production in some of the engineered strains, we quantified the expression levels of all Kivd variants *via* Western-immunoblotting using antibody against Strep-tag since all the Kivd variants were Strep-tagged on their N-terminals. We observed significant differences on Kivd expression levels in all of these engineered *Synechocystis* strains (Fig. 2B). The decreased expression of several engineered Kivd proteins may be due to their instability, low solubility, or some harmful effects exerted by the modified protein on the host cell (Miroux and Walker, 1996; Dumon-Seignovert et al., 2004). It has been demonstrated that improving core packing, surface polarity, and backbone rigidity can increase the stability and solubility of heterologous overexpressed proteins in *E. coli* (Goldenzweig et al., 2016). Thus, further mutations could be investigated on Kivd to overcome these difficulties. Furthermore, extremely high activity or product toxicity may also cause difficulties for the protein to be correctly expressed (Rosano and Ceccarelli, 2014). A case was reported when Higashide et al. (2011) tried to overexpress the α-acetolactate synthase (AlsS) from *Bacillus subtilis* (*B. subtilis*) in *C. cellulyticum*. It was suggested in that study, a tunable inducible promoter with large regulation range may help to overcome this problem.

The Kivd variants VL, VF, and VA showed extremely different performance in *Synechocystis* compared to their performance in *E. coli* (Zhang et al., 2008; Chen et al., 2017). The engineered *E. coli* strains showed the production of target compounds, which indicate that these Kivd variants were expressed and functioning in the host cells even though the expression level was not examined. In this present study, strain VL did not show any production of either product and no Kivd expression could be detected, while the other five engineered strains (MV, VF, VA, FL, and QW) did not give any production even with considerable Kivd expression level (Fig. 2). This inactivity could be caused by incomplete folding which means that the proteins formed a soluble conformation but the structure of the active site was too perturbed to give enzymatic activity (González-Montalbán et al., 2007). In some cases, the addition of small molecules, *e.g.* metals, and relatively lower environmental temperature may be needed to overcome this problem (Yang et al., 2003). Thus, all the differences between the results from *E. coli* and *Synechocystis* prove the importance of investigating the *in vivo* performance of the enzyme of interest in the target host cell, since the results could be extremely different.

3.3. Further investigation on the selected strains

Since in this study, we mainly focused on investigating the *in vivo* performance of the engineered enzyme for enhancing isobutanol production in *Synechocystis*, the evaluation of different engineered Kivd variants was based on several intracellular factors, *e.g.* protein expression level, *in vivo* substrate competition, and isobutanol production per same amount of protein.

Based on the preliminary results above (Fig. 2), we selected strains Original, VI, ST and SV for further investigation and the relative expression levels of Kivd in all 4 strains were quantified through further Western-immunoblot experiments. Using the intensities of the bands from Western-immunoblots (Fig. 3B), we normalized the expression level of the original Kivd to 1, and the Kivd relative expression from VI, ST and SV resulted in 1.12, 1.27, and 0.31, respectively (Fig. 3C).

All these four selected strains were cultivated for 8 days since the culture turned unhealthy thereafter and stopped producing isobutanol and 3M1B. The original strain grew faster than the others while strain SV grew the least during the 8 days of cultivation (Fig. 4A). It is highly unlikely that the retarded growth of these engineered Kivd strains was caused by the amounts of isobutanol or 3M1B that was actually

produced, since cyanobacteria have been shown to have a much higher tolerance to *e.g.* isobutanol (Atsumi et al., 2009). Further investigation needs to be done in the future to find out the real reason for this phenotype.

Strains VI and ST had similar growth curves, especially during the log phase. Isobutanol titer increased from day 2 to day 8 in all the strains and strain ST produced the most, $59.6\,\mathrm{mg\,L^{-1}}$ isobutanol and $18.2\,\mathrm{mg\,L^{-1}}$ 3M1B while strain SV only produced trace amounts of both products, $5.6\,\mathrm{mg\,L^{-1}}$ and $1\,\mathrm{mg\,L^{-1}}$, respectively (Fig. 4B). Interestingly, the rate of increase in isobutanol titer in all the strains follow the trend of their respective growth rate. For instance, strain ST produced approximately $12.6\,\mathrm{mg\,L^{-1}}$ isobutanol per day in the log phase (day 2–4) while in the stationary phase (day 4–8), it produced around $7.02\,\mathrm{mg\,L^{-1}}$ isobutanol per day. No further increase in the isobutanol titer was detected from day 8 to day 10 (data not shown). Therefore, it means that more isobutanol can be synthesized when more biomass is accumulated. The reason may be that the root of isobutanol synthesis pathway is the valine synthesis pathway. When the cells are under maximum specific growth rate, there is high intracellular demand of amino acid and carbon flux towards this direction increases, so that in the presence of Kivd, isobutanol production also increases. In a future study, it would be interesting to create a bio-switch between amino acid synthesis and isobutanol synthesis, or to use cells under constant log phase condition.

Since we could observe differences in the growth curves, the production of each mutated strain on day 4 (last day of log phase) was compared with that of the original strain in order to remove this bias due to the different cell concentrations. As expected, VI and ST produced $9.72\,\mathrm{mg\,L^{-1}\,OD_{750}^{-1}}$ and $10.59\,\mathrm{mg\,L^{-1}\,OD_{750}^{-1}}$ isobutanol, respectively, which are more than 3 times higher than the production of $3.2\,\mathrm{mg\,L^{-1}\,OD_{750}^{-1}}$ from the original strain (Fig. 4C). Then, we quantified the isobutanol-to-3M1B molar ratio from all the strains (Fig. 4D) on day 8. Strains VI, ST, and SV showed statistically significant increase of isobutanol-to-3M1B molar ratio compared to that of the original strain. Notably, the increase in ratio was the greatest in the strain SV, which showed a 2.4-fold increase compared to that for the original strain. This result quantitatively shows that the application of combined mutation S286T/Val461I affects the preferential shift of Kivd towards isobutanol production more significantly compared to the single mutations. Unfortunately, the overall production from this combined strain was very limited even though the isobutanol-to-3M1B molar ratio in this strain was the highest.

Regarding the reason of the low production of isobutanol from strain SV, two hypotheses were made: i) that this Kivd has the same or higher activity compared to the original Kivd, so that the low production was solely due to the low protein expression level, and ii) that the low production was a result of both decrease in Kivd activity and low protein expression level. To answer this question, we calculated the *in vivo* isobutanol production per specific unit of Kivd protein, as a way to estimate the relative *in vivo* activity of Kivd towards the substrate (Fig. 5A). We also performed *in vitro* activity assays using KIV as substrate on crude extracted protein, and the activities were normalized according to the relative expression level of the corresponding Kivd (Fig. 5B). The relative *in vivo* activity of SV showed no significant difference compared to that of the original Kivd while the relative *in vitro* activity of SV was 1.2 times higher than the original Kivd. Thus, the first hypothesis was confirmed, namely that the low isobutanol production of strain SV was only due to the low Kivd expression level, and not due to the decrease of activity towards the substrate KIV. In order to investigate more directly the changes in the isobutanol-to-3M1B molar ratios across these Kivd strains, their *in vivo* activities towards KIC (the substrate for 3M1B production) was also estimate through measurements of 3M1B production (Fig. 5C). Comparing the results in Fig. 5A and C, it can be seen that both VI and ST showed increased activity towards both isobutanol production and 3M1B production. However, the increase of activity towards isobutanol production (around 3-fold)
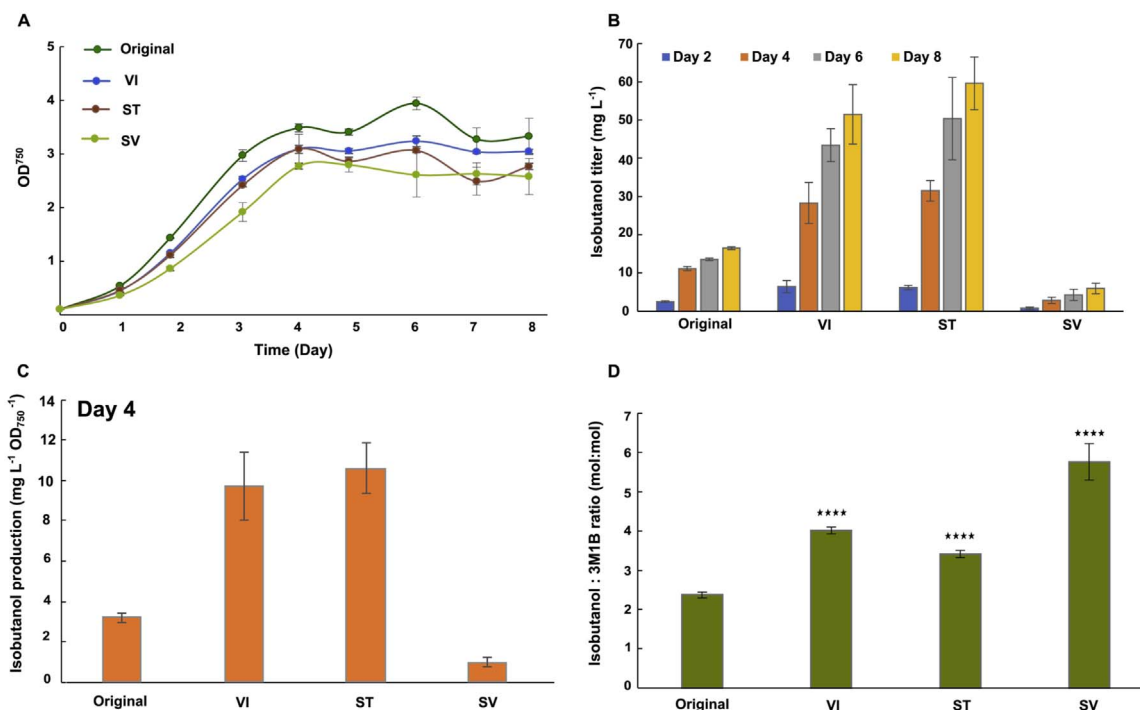
Fig. 4. Growth, isobutanol production, and products' molar ratio of the selected engineered *Synechocystis* PCC 6803 strains. A) Growth curves of the selected strains. Optical density was measured every day using micro-plate reader. B) Isobutanol titer from different strains on day 2, day 4, day 6 and day 8. C) Isobutanol production from different strains on day 4. D) Molar ratio of isobutanol and 3-methyl-1-butanol produced in different strains, calculated based on the titer on day 8. Asterisks represent significant differences between the corresponding strain and the original strain, **** = p < 0.0001 in *t*-test. All the results represent the mean of two technical replicates with three biological replicates, error bars represent the standard deviation.

was higher than the increase of activity towards 3M1B production (1.6-fold). Therefore, it could be confirmed that the higher isobutanol-to-3M1B molar ratio in these two strains (Fig. 4D) was due to the higher enhancement of activity towards KIV in comparison to KIC as the substrate. Interestingly, SV showed in fact half the activity towards KIC than the original Kivd, while its activity towards KIV for isobutanol production was essential unaffected. This demonstrates that, in SV, the higher isobutanol-to-3M1B molar ratio is now solely due to decreased activity towards KIC as a substrate, leading to reduced 3M1B production relative to expressed protein. If the expression of this mutated Kivd can be regulated precisely and enhanced in *Synechocystis*, SV could be an ideal strain that has the most preferential shift towards isobutanol production.

4. Conclusion

This is the first study focusing on engineering protein for increasing the production of specific compound in *Synechocystis* and the evaluation of these proteins based on detailed analyses of their *in vivo* performance. In this work, we have successfully enhanced isobutanol titer and production in *Synechocystis* by engineering Kivd, one of the bottleneck enzymes, to have higher *in vivo* and *in vitro* activity towards substrate KIV that leads to isobutanol formation. The substitution of Val461 and Ser286 to isoleucine and threonine, respectively, showed more than three times the production of isobutanol compare with the original Kivd strain, and an increase of isobutanol-to-3M1B molar ratio was observed as well. The combined modified strain SV containing V461I/S286T showed highest isobutanol-to-3M1B molar ratio in the mixture of the
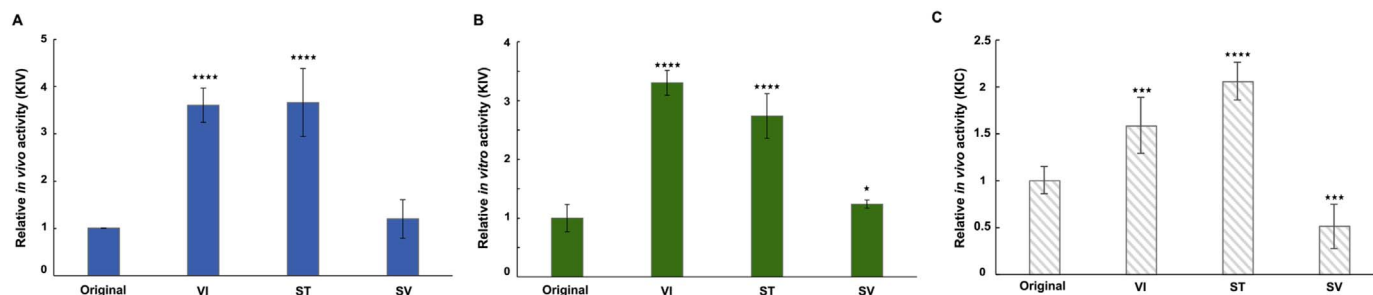

Fig. 5. Relative *in vivo* (in *Synechocystis* PCC 6803) and *in vitro* activity from different Kivd using substrate KIV and relative *in vivo* activity of different Kivd using substrate KIC. A) Relative *in vivo* activity using KIV as substrate. Relative activity in *Synechocystis* engineered strain equals to isobutanol production (mg L^{-1} OD^{-1}) divided by the relative protein expression level. B) Relative *in vitro* activity using KIV as substrate. Crude extract protein from each strain was used in the *in vitro* assay and the concentrations were normalized to a same amount for all the reactions. Then the relative activity was calculated based on the relative Kivd expression level in different strains. It represents the relative NADH consumption in a certain time per same amount of Kivd protein. C) Relative *in vivo* activity using KIC as substrate. Relative activity in *Synechocystis* engineered strain equals to 3M1B production (mg L^{-1} OD^{-1}) divided by the relative protein expression level. Asterisks represent significant differences between the corresponding strain and the original strain, * = p < 0.05*** = 0.0001 < p < 0.001**** = p < 0.0001 in *t*-test. All the results represent the mean of two technical replicates per two biological replicates. The relative activities in each panel was calculated using the relative protein expression level for each biological replicate and the isobutanol/3M1B production (panel A & C) or NADH consumption (panel B) in the corresponding sample. The error bars represent the standard deviation of these calculated values.

final products. However, this strain showed the lowest total production for both products, which was due to the extremely low expression level of the engineered Kivd. Therefore, it has been shown clearly in this study that a single amino acid substitution can significantly affect the expression level and the function of a protein in *Synechocystis*, hence, protein engineering is a powerful tool for modifying the output of metabolic pathway.

Acknowledgements

DeclarationsAuthors' contribution

RM designed the project and performed most of the experiments, analysed the data and wrote the manuscript. HX performed part of the experiments. FH supervised the project and revised the manuscript. PL is the main supervisor for this project and revised the manuscript. All the authors read and approved the final version of the manuscript.Availability of data and materials

The datasets used and/or analysed during the current study available from the corresponding author on reasonable request.Competing interests

The authors declare that they have no competing interests.

Appendix A. Supporting information

Supplementary data associated with this article can be found in the online version at http://dx.doi.org/10.1016/j.ymben.2018.02.014.

References

Arnold, F.H., 1993. Engineering proteins for nonnatural environments. FASEB J. 7, 744–749.

Arnold, F.H., Volkov, A.A., 1999. Directed evolution of biocatalysts. Curr. Opin. Chem. Biol. 3, 54–59.

Atsumi, S., Higashide, W., Liao, J.C., 2009. Direct photosynthetic recycling of carbon dioxide to isobutyraldehyde. Nat. Biotechnol. 27, 1177–1180.

Baez, A., Cho, K.-M., Liao, J.C., 2011. High-flux isobutanol production using engineered *Escherichia coli*: a bioreactor study with in situ product removal. Appl. Microbiol. Biotechnol. 90, 1681–1690.

Berthold, C.L., Gocke, D., Wood, M.D., Leeper, F.J., Pohl, M., Schneider, G., 2007. Structure of the branched-chain keto acid decarboxylase (KdcA) from *Lactococcus lactis* provides insights into the structural basis for the chemoselective and enantioselective carboligation reaction. Acta Crystallogr. D Biol. Crystallogr. D 63, 1217–1224.

Breslow, R., 1957. Rapid deuterium exchange in thiazolium salts. J. Am. Chem. Soc. 79, 1762–1763.

Chen, G.S., Siao, S.W., Shen, C.R., 2017. Saturated mutagenesis of ketoisovalerate decarboxylase V461 enabled specific synthesis of 1-pentanol via the ketoacid elongation cycle. Sci. Rep. 7, 11284.

Chew, K.W., Yap, J.Y., Show, P.L., Suan, N.H., Juan, J.C., Ling, T.C., Lee, D.-J., Chang, J.-S., 2017. Microalgae biorefinery: high value products perspectives. Bioresour. Technol. 229, 53–62.

Dobritzsch, D., König, S., Schneider, G., Lu, G., 1998. High resolution crystal structure of pyruvate decarboxylase from *Zymomonas mobilis* implications for substrate activation in pyruvate decarboxylases. J. Biol. Chem. 273, 20196–20204.

Du, J., Shao, Z., Zhao, H., 2011. Engineering microbial factories for synthesis of value-added products. J. Ind. Microbiol. Biotechnol. 38, 873–890.

Du, J., Yuan, Y., Si, T., Lian, J., Zhao, H., 2012. Customized optimization of metabolic pathways by combinatorial transcriptional engineering. Nucleic Acids Res. 40 e142.

(e142–e142).

Dumon-Seignovert, L., Cariot, G., Vuillard, L., 2004. The toxicity of recombinant proteins in *Escherichia coli*: a comparison of overexpression in BL21(DE3), C41(DE3), and C43(DE3). Protein Expr. Purif. 37, 203–206.

Eriksen, D.T., Lian, J., Zhao, H., 2014. Protein design for pathway engineering. J. Struct. Biol. Des. Protein Funct. 185, 234–242.

Frank, R.A.W., Leeper, F.J., Luisi, B.F., 2007. Structure, mechanism and catalytic duality of thiamine-dependent enzymes. Cell. Mol. Life Sci. 64, 892.

Goldenzweig, A., Goldsmith, M., Hill, S.E., Gertman, O., Laurino, P., Ashani, Y., Dym, O., Unger, T., Albeck, S., Prilusky, J., Lieberman, R.L., Aharoni, A., Silman, I., Sussman, J.L., Tawfik, D.S., Fleishman, S.J., 2016. Automated structure- and sequence-based design of proteins for high bacterial expression and stability. Mol. Cell 63, 337–346.

González-Montalbán, N., García-Fruitós, E., Villaverde, A., 2007. Recombinant protein solubility - does more mean better? Nat. Biotechnol. 25, 718–720.

Higashide, W., Li, Y., Yang, Y., Liao, J.C., 2011. Metabolic engineering of *Clostridium cellulolyticum* for production of isobutanol from cellulose. Appl. Environ. Microbiol. 77, 2727–2733.

Huang, H.-H., Camsund, D., Lindblad, P., Heidorn, T., 2010. Design and characterization of molecular tools for a Synthetic Biology approach towards developing cyanobacterial biotechnology. Nucleic Acids Res. 38, 2577–2593.

Jazmin, L.J., Xu, Y., Cheah, Y.E., Adebiyi, A.O., Johnson, C.H., Young, J.D., 2017. Isotopically nonstationary 13C flux analysis of cyanobacterial isobutyraldehyde production. Metab. Eng. 42, 9–18.

Kern, D., Kern, G., Neef, H., Tittmann, K., Killenberg-Jabs, M., Wikner, C., Schneider, G., Hübner, G., 1997. How thiamine diphosphate is activated in enzymes. Science 275, 67–70.

Kluger, R., 1987. Thiamin diphosphate: a mechanistic update on enzymic and nonenzymic catalysis of decarboxylation. Chem. Rev. 87, 863–876.

Lee, S.Y., Kim, H.U., 2015. Systems strategies for developing industrial microbial strains. Nat. Biotechnol. 33, 1061–1072 (nbt).

Li, X., Shen, C.R., Liao, J.C., 2014. Isobutanol production as an alternative metabolic sink to rescue the growth deficiency of the glycogen mutant of *Synechococcus elongatus* PCC 7942. Photosynth. Res. 120, 301–310.

Miao, R., Liu, X., Englund, E., Lindberg, P., Lindblad, P., 2017. Isobutanol production in *Synechocystis* PCC 6803 using heterologous and endogenous alcohol dehydrogenases. Metab. Eng. Commun. 5, 45–53.

Milne, N., van Maris, A.J.A., Pronk, J.T., Daran, J.M., 2015. Comparative assessment of native and heterologous 2-oxo acid decarboxylases for application in isobutanol production by *Saccharomyces cerevisiae*. Biotechnol. Biofuels 8, 204.

Miroux, B., Walker, J.E., 1996. Over-production of proteins in *Esherichia coli*: mutant hosts that allow synthesis of some membrane proteins and globular proteins at high levels. J. Mol. Biol. 260, 289–298.

Nair, N.U., Zhao, H., 2008. Evolution in reverse: engineering a D-xylose-specific xylose reductase. ChemBioChem 9, 1213–1215.

Nowroozi, F.F., Baidoo, E.E.K., Ermakov, S., Redding-Johanson, A.M., Batth, T.S., Petzold, C.J., Keasling, J.D., 2014. Metabolic pathway optimization using ribosome binding site variants and combinatorial gene assembly. Appl. Microbiol. Biotechnol. 98, 1567–1581.

Nozzi, N.E., Oliver, J.W.K., Atsumi, S., 2013. Cyanobacteria as a platform for biofuel production. Synth. Biol. 1, 7.

Redding-Johanson, A.M., Batth, T.S., Chan, R., Krupa, R., Szmidt, H.L., Adams, P.D., Keasling, J.D., Soon Lee, T., Mukhopadhyay, A., Petzold, C.J., 2011. Targeted proteomics for metabolic pathway optimization: application to terpene production. Metab. Eng. 13, 194–203.

Rippka, R., Deruelles, J., Waterbury, J.B., Herdman, M., Stanier, R.Y., 1979. Generic assignments, strain histories and properties of pure cultures of cyanobacteria. Microbiology 111, 1–61.

Rosano, G.L., Ceccarelli, E.A., 2014. Recombinant protein expression in Escherichia coli: advances and challenges. Front. Microbiol. 5, 172.

Shen, C.R., Liao, J.C., 2012. Photosynthetic production of 2-methyl-1-butanol from CO 2 in cyanobacterium *Synechococcus elongatus* PCC7942 and characterization of the native acetohydroxyacid synthase. Energy Environ. Sci. 5, 9574–9583.

Tsuge, T., Hisano, T., Taguchi, S., Doi, Y., 2003. Alteration of chain length substrate specificity of *Aeromonas caviae* R-enantiomer-specific enoyl-coenzyme A hydratase through site-directed mutagenesis. Appl. Environ. Microbiol. 69, 4830–4836.

Varman, A.M., Xiao, Y., Pakrasi, H.B., Tang, Y.J., 2013. Metabolic engineering of Synechocystis sp. Strain PCC 6803 for isobutanol production. Appl. Environ. Microbiol. 79, 908–914.

Xiong, M., Deng, J., Woodruff, A.P., Zhu, M., Zhou, J., Park, S.W., Li, H., Fu, Y., Zhang, K., 2012. A bio-catalytic approach to aliphatic ketones. Sci. Rep. 2, srep00311.

Yang, Q., Xu, J., Li, M., Lei, X., An, L., 2003. High-level expression of a soluble snake venom enzyme, gloshedobin, in *E. coli* in the presence of metal ions. Biotechnol. Lett. 25, 607–610.

Yep, A., Kenyon, G.L., McLeish, M.J., 2006. Determinants of substrate specificity in KdcA, a thiamin diphosphate-dependent decarboxylase. Bioorg. Chem. 34, 325–336.

Zha, W., Shao, Z., Frost, J.W., Zhao, H., 2004. Rational pathway engineering of type I fatty acid synthase allows the biosynthesis of triacetic acid lactone from D-glucose in vivo. J. Am. Chem. Soc. 126, 4534–4535.

Zhang, K., Sawaya, M.R., Eisenberg, D.S., Liao, J.C., 2008. Expanding metabolism for biosynthesis of nonnatural alcohols. Proc. Natl. Acad. Sci. USA 105, 20653–20658.